

## The Influence of X-ray Polarization on the Visibility of Pendellösung Fringes in X-ray Diffraction Topographs

BY M. HART\* AND A. R. LANG

*H. H. Wills Physics Laboratory, Royal Fort, Bristol, England*

(Received 3 November 1964)

The visibility of Pendellösung fringes is found to vary periodically with the fringe order. This variation of fringe visibility can be explained by the dynamical theory of X-ray diffraction taking into account the unpolarized nature of the incident X-ray beam. It has been experimentally demonstrated that there is no modulation in fringe visibility if the incident X-ray beam is approximately plane-polarized.

### Introduction

The first observations of Pendellösung fringes in the X-ray case were made by Kato & Lang (1959) in the diffraction topographs of wedge-shaped regions of fairly perfect crystals. They prepared wedge-shaped specimens of silicon and quartz and were able to show that the spacing of the Pendellösung fringes was inversely proportional to the structure factor of the Bragg reflexion used to obtain the diffraction topograph.

In a series of experiments during which diffraction topographs of silicon and germanium wedge-shaped specimens were obtained with silver, molybdenum, or copper  $K\alpha_1$  radiation, we have noticed that the visibility of Pendellösung fringes varies periodically with the fringe order. We have demonstrated, by two different methods, that these variations in fringe visibility occur as a result of the superposition of two sets of fringes with different spacings. One set of fringes is due to X-rays which are plane-polarized with the electric vector normal to the plane defined by the incident and diffracted X-ray beams, while the other set of fringes is due to X-rays which are plane polarized with the electric vector lying in that plane.

### Experimental

#### Experimental technique

In most of the experiments, the apparatus was the same as that used previously in studies of individual dislocations by transmission X-ray diffraction topography (Lang, 1959). The principle of the method is shown in Fig. 1. The X-ray beam is collimated by a slit system and the crystal  $C$  is set to satisfy the Bragg condition for a particular characteristic radiation.  $S$  is a slit in a lead screen through which only the diffracted beam may pass to reach the recording film  $F$ . The specimen and film are moved together past the incident beam so that we can record on the film a diffraction topograph from a large area of the crystal.

In this case it is assumed that the incident beam of X-rays is unpolarized.

When copper  $K\alpha_1$  radiation was used, the incident X-ray beam could be almost plane-polarized with the electric vector lying in the plane of the ribbon beam by symmetric Bragg reflexion in the third order from a  $\{111\}$  face of the perfect germanium crystal ( $P$  in Fig. 2). The Bragg angle of the 333 reflexion from germanium with copper  $K\alpha_1$  radiation is very close to  $45^\circ$ .

In both experimental arrangements the divergence of the beam incident upon  $C$  was sufficient to ensure

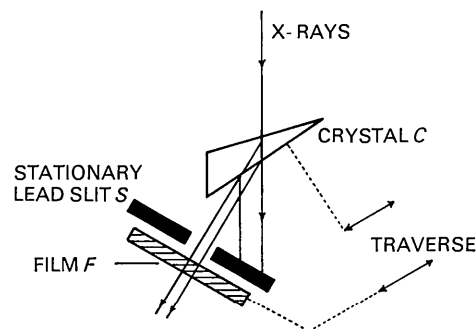


Fig. 1. Experimental arrangement using unpolarized incident beam, explained in text.

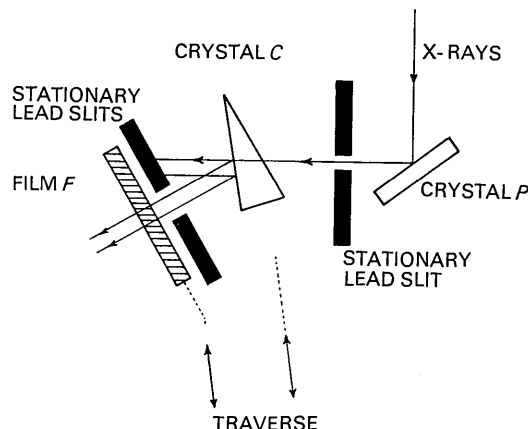


Fig. 2. Experimental arrangement using a plane polarized incident beam, explained in text.

\* Present address: Engineering Physics and Materials Science, Bard Hall, Cornell University, Ithaca, N.Y., U.S.A.

that the image recorded was a topographic record of the integrated reflexion from the wedge-shaped crystal *C*.

#### Specimen preparation

Wedge-shaped germanium and silicon specimens were prepared from nominally dislocation-free material. In each case one surface was close to (111) and the wedge edge was parallel to the  $[\bar{1}10]$  direction. The wedges were approximately 1 cm square, the maximum thickness being 0.5 mm. in the case of the germanium wedge (specimen *A*) and 4 mm for the silicon wedge (specimen *B*). After careful grinding the crystals were chemically polished to remove damaged surface layers. Germanium was chemically polished in a mixture of concentrated nitric and hydrofluoric acids in the ratio of 10 to 1 parts respectively by volume, while silicon was chemically polished in CP-4 (5 parts nitric acid, 3 parts hydrofluoric acid, 3 parts acetic acid and 0.2 parts bromine).

Spurious intensity variations on the topographs due to non-uniformity of the thickness gradient of the wedges were avoided by making a direct check of the uniformity of the wedges after chemical polishing had been completed. The transmitted intensity of a harmonic-free, crystal-monochromatized X-ray beam was measured as a function of distance from the edge of the wedge. The X-ray beam was 1 mm by 25 microns in cross section, the long dimension being parallel to the edge of the wedge. Copper  $K\alpha_1$  radiation was used for specimen *A* and molybdenum  $K\alpha_1$  for specimen *B*. In both cases the rate of increase of wedge thickness with distance from the edge of the wedge was found to be sufficiently uniform for our purpose.

#### Experimental results

We have recorded many different projection topographs of the two crystal wedges, some of which are illustrated in Figs. 3-6. The microdensitometer traces, obtained from the projection topographs, show directly how the integrated reflecting power of a perfect crystal varies with crystal thickness. The recording medium was Ilford L4 nuclear emulsion and the microdensitometer traces were made with a Joyce, Loebel Mk III recording microdensitometer. Preliminary experiments showed that with the emulsion processing technique we adopted the optical density of the emulsion was proportional to the X-ray dose up to an optical density of 2.5.

Fig. 3 is the microdensitometer trace of the diffraction topograph of specimen *A* obtained with the  $11\bar{1}$  reflexion and unpolarized copper  $K\alpha_1$  radiation. We observe that the fifth fringe, which is indicated by an arrow, has anomalously low visibility. Fig. 4 shows the  $\bar{2}20$  diffraction topograph of specimen *A* taken with unpolarized copper  $K\alpha_1$  radiation. In this case, positions of minimum fringe visibility occur at intervals of approximately 2.5 fringes. When the incident radiation is plane-polarized with the electric vector normal to the

plane defined by the incident and diffracted beam directions, as in Fig. 5, the modulation of Pendellösung fringe visibility is absent. The slight increase in background density near the ninth fringe is due to fluorescence from the polarizing crystal *P* which passed through both lead slits. As a further example, Fig. 6 shows the microdensitometer trace of the  $\bar{2}20$  diffraction topograph of specimen *B* taken with unpolarized molybdenum  $K\alpha_1$  radiation. In this case we see many Pendellösung fringes because the linear absorption coefficient of silicon for molybdenum  $K\alpha_1$  radiation is low; the minima of fringe visibility occur at intervals of 14 fringes.

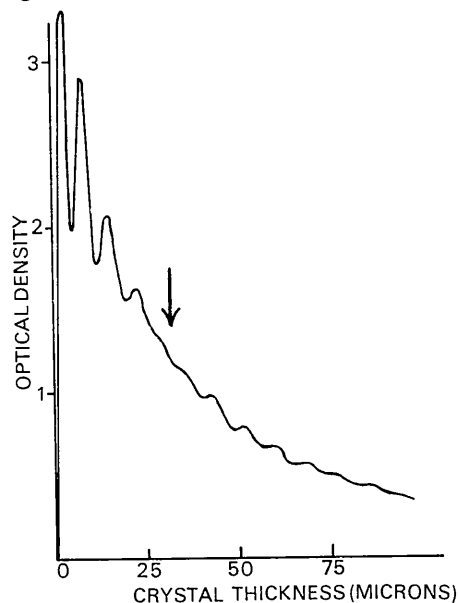


Fig. 3. Photometer trace of topograph of germanium wedge,  $11\bar{1}$  reflexion,  $\text{Cu } K\alpha_1$  radiation.

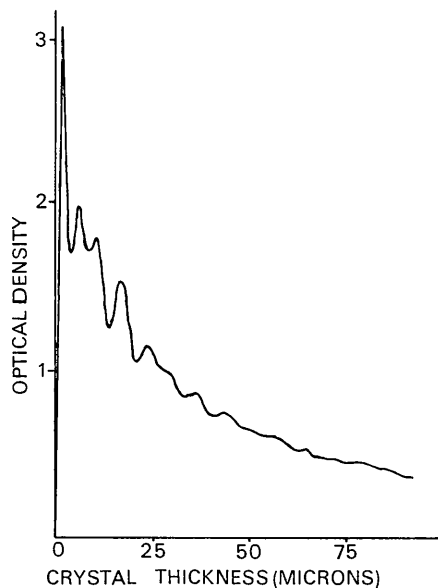


Fig. 4. Photometer trace of topograph of germanium wedge,  $\bar{2}20$  reflexion,  $\text{Cu } K\alpha_1$  radiation.

### Theory

The dynamical theory of X-ray diffraction applied to the case where the incident beam is unpolarized (see e.g. James, 1963), and only one Bragg reflexion is excited, shows that the dispersion surface has four branches. The four branches form a pair of hyperbolae with the same asymptotes but with their diameters in the ratio of  $|\cos 2\theta|$  to 1, where  $\theta$  is the Bragg angle. When the incident radiation is plane-polarized with the electric vector either in or normal to the plane defined by the directions of the incident and diffracted rays, the dispersion surface consists of only one of these hyperbolae. The dispersion hyperbola with the larger diameter corresponds to the case when the electric vector is normal to the plane containing both the incident and diffracted beam directions.

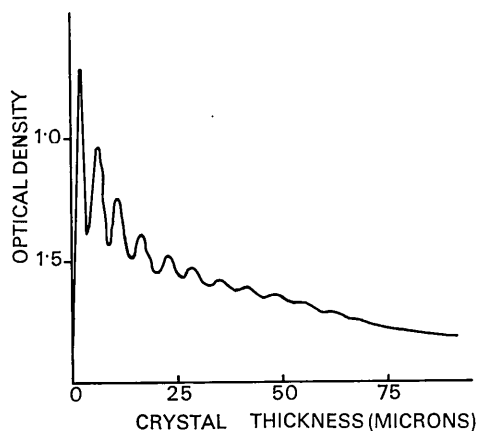


Fig. 5. Photometer trace of topograph of germanium wedge,  $\bar{2}20$  reflexion, plane-polarized  $\text{Cu } K\alpha_1$  radiation.

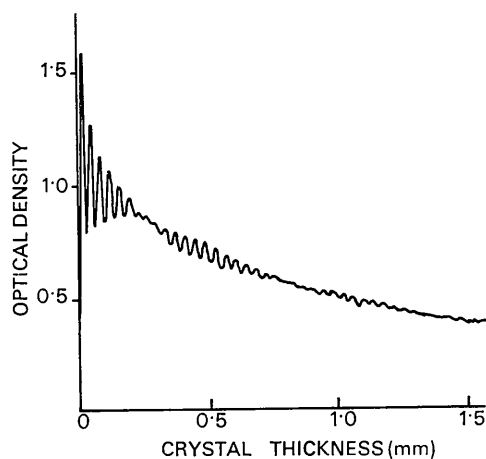


Fig. 6. Photometer trace of topograph of silicon wedge,  $\bar{2}20$  reflexion,  $\text{Mo } K\alpha_1$  radiation.

Kato (1961) has shown that, except for the low order fringes, the spacing of Pendellösung fringes in projection topographs is inversely proportional to the minimum diameter of the dispersion surface. Thus, when the incident radiation is unpolarized, the projection topograph consists of two superimposed sets of fringes with different spacings, corresponding to the two principal directions of polarization.

If we approximate the intensity profiles of both sets of Pendellösung fringes by the same sinusoidal function it follows straightforwardly that the projection topograph should show fringes with a spacing which is inversely proportional to the mean diameter of the two dispersion surfaces. However, the visibility of the fringes should vary periodically with fringe order, being small at intervals of  $\frac{1}{2}(2n+1)N$  fringes, where  $n$  is a positive integer or zero and

$$N = \frac{1}{2}(1 + |\cos 2\theta|)/(1 - |\cos 2\theta|). \quad (1)$$

The positions of the minima of fringe visibility thus depend only on the Bragg angle of the reflexion involved. A comparison between the observed and calculated positions of minimum fringe visibility is shown in Table 1.

Let us consider the actual intensity profile of the wedge topographs more closely. The early experiments of Kato & Lang (1959) showed that the assumption that the wave incident upon the crystal was a plane wave (which assumption is used in the development of dynamical X-ray diffraction theory as given by Ewald, von Laue & Zachariasen) was not adequate to explain the Pendellösung fringe patterns in section topographs of crystals taken with the usual experimental arrangements. Instead of a plane wave, a coherent spherical incident wave is required to account for such patterns. The spherical-wave theory has been developed thoroughly by Kato (1961). In this study Kato showed *inter alia* that for the *integrated* intensities of *projection* topographs the plane-wave theory and the spherical-wave theory make similar predictions. Thus we may use the values calculated for the Laue (transmission) geometry given by Zachariasen (1945) for a non-absorbing specimen, and by Ramachandran (1954) and Kato (1955) for an absorbing specimen.

The diffraction geometry of the gently tapering wedges with which we are here concerned is sufficiently close to that of the parallel-sided plate used in symmetrical transmission to allow us to apply the simple expressions derived for the latter case. In so doing we will modify slightly the familiar formulae in order to display the effect of the state of polarization of the incident beam.

Table 1. Positions of minimum fringe visibility

Specimen	Radiation	Reflexion	$N$ calc	$N$ observed
<i>A</i>	Copper $K\alpha_1$	$11\bar{1}$	8.4	$\frac{1}{2}N=4.5$
<i>A</i>	Copper $K\alpha_1$	$\bar{2}20$	2.5	2.5
<i>B</i>	Molybdenum $K\alpha_1$	$\bar{2}20$	14	14

Let  $D$  denote the minimum diameter of the dispersion surface for waves polarized with the electric vector perpendicular to the plane of incidence ( $\sigma$  case). Then for waves with electric vector parallel to the plane of incidence ( $\pi$  case) the minimum diameter of the dispersion surface is  $CD$ , where  $C = |\cos 2\theta|$ . In terms of familiar quantities, we have

$$D = \left( \frac{e^2}{mc^2} \right) \frac{\lambda F}{\pi V \cos \theta},$$

$F$  being the structure amplitude and  $V$  the volume of the unit cell.

For a crystal of thickness  $t$ , in the symmetrical Laue case, and with negligible absorption, the integrated reflexion  $R$  from Bragg planes of interplanar spacing  $d$  is given by

$$R = \frac{1}{4} \pi D d \left[ \int_0^{2\pi t D} J_0(x) dx + C \int_0^{2\pi t C D} J_0(x) dx \right]. \quad (2)$$

The first and second terms in the parenthesis of equation (2) represent the contributions of the  $\sigma$  and  $\pi$  waves, respectively. The integrals have been graphed by Zachariassen (1945) and by von Laue (1960). For Pendellösung fringes of higher order than the first few, the asymptotic expressions for the Bessel functions may be used. Equation (2) then becomes

$$R = \frac{1}{4} \pi D d \left[ 1 + C + (2/\pi X)^{\frac{1}{2}} \sin(X - \pi/4) + (2C/\pi X)^{\frac{1}{2}} \sin(CX - \pi/4) \right] \quad (3)$$

in which  $X$  stands for  $2\pi t D$ . From this equation the expression for the periodicity of fringe visibility, equation (1), follows directly. We see, moreover, that the ratio of the amplitudes of the oscillatory terms is  $C^{\frac{1}{2}}$ . This differs from unity by less than 10% for values of  $2\theta$  below  $35^\circ$ . Thus with the low Bragg angles commonly used in topographs taken with Mo  $K\alpha$  or Ag  $K\alpha$  radiation the Pendellösung fringes disappear completely at the minima of fringe visibility.

When the product of linear absorption coefficient,  $\mu$ , and crystal thickness,  $t$ , is such that  $\mu t > 1$  then the formulae of Ramchandran (1954) or Kato (1955) should be used for the integrated reflexion. In the symmetrical Laue case their formulae may be written

$$R = \frac{1}{4} \pi D d \exp(-\mu t \sec \theta) \left[ I_0(\kappa X) - 1 + \int_0^X J_0(x) dx + C \{ I_0(C\kappa X) - 1 + \int_0^{CX} J_0(x) dx \} \right]. \quad (4)$$

In this expression  $I_0$  is the modified Bessel function of the first kind, and  $\kappa$  is the ratio of the imaginary to the real part of the centrosymmetric structure amplitude (equation 3.179, Zachariassen 1945). The functions  $I_0$  represent the enhanced transmitted diffracted intensity that appears in the vicinity of Bragg reflexion, *i.e.* the Borrmann effect. Owing to the presence of these terms the relative modulation of the diffracted intensity by Pendellösung fringes is less than in the non-absorbing case, equation (2). However, it is interesting to note

that the oscillatory components of  $R$ , both for  $\sigma$  and  $\pi$  waves, have the normal attenuation coefficient,  $\exp(-\mu t \sec \theta)$ . Hence the pattern of superimposed Pendellösung fringes due to the  $\sigma$  and  $\pi$  waves is independent of  $\kappa$  and differs only from that of the non-absorbing crystals by the presence of the normal exponential attenuation.

### Discussion

The good agreement between experiment and theory demonstrates the validity of the dynamical theory of diffraction in highly perfect crystals such as our specimens. In addition, the factors discussed above have implications in several directions, which we will now consider separately.

### Intensity measurements

The equations show that if the integrated intensity of a thin or fairly thin perfect crystal used in transmission is to be calculated correctly the contributions of the  $\sigma$  and  $\pi$  waves must be computed separately and then added together. If  $N=5$ , say, errors up to about 20% in the integrated intensity could be introduced by the simpler calculation procedure of inserting a mean polarization factor into a single expression of the form  $\int_0^X J_0(x) dx$ .

### The polarization ratio

Experiments have shown that crystals containing an appreciable dislocation density, ranging up to  $10^4$  to  $10^5$  lines per  $\text{cm}^2$ , or a high density of precipitates of sub-micron size (*e.g.* nitrogen platelets in diamond) can still possess sufficient long-range regularity of lattice repeat to show quite good visibility of Pendellösung fringes, and, when higher Bragg angles are used, a periodicity of fringe visibility such as that here reported. It follows that if a fairly perfect crystal has a plate-like habit, or has any appreciable part with roughly constant thickness not greater than, say, a few times the reciprocal of  $D$  (*i.e.* of order a few extinction distances) then the ratio of intensities of  $\pi$  waves and  $\sigma$  waves in the diffracted beam may depart considerably in either sense from  $|\cos 2\theta|:1$ . Now it has been already recognized (Parthasarathy, Ramchandran & Mallikarjunan, 1963) that in absorbing crystals the polarization ratio  $\alpha$ , *i.e.* the ratio of integrated reflexion of  $\pi$  waves to that of  $\sigma$  waves, can fall much lower than the mosaic crystal limit  $\cos^2 \theta$ . This is made clear by equation (4) above, which shows that for a sufficiently thick crystal the term  $I_0(\kappa X)$  in the  $\sigma$ -wave contribution will become the dominant one in the whole expression. Thus for absorbing crystals in which some or all of the diffracted beam is transmitted through the crystal the polarization ratio  $\alpha$  does not offer an unambiguous 'perfection index' for the crystal. We see now, moreover, that for crystals sufficiently thin to be negligibly absorbing the value of  $\alpha$  is still an ambiguous quantity, as a result of the different periodicity of the oscillatory terms in the

contributions of  $\sigma$  and  $\pi$  waves to the integrated reflection.

*Pendellösung fringe visibility as a crystal perfection index*

We have for some years used the visibility of Pendellösung fringes in a very qualitative way as an indicator of crystal perfection. This type of observation appears capable of development as a quantitative technique. In crystals of low dislocation density the modulation of the total diffracted intensity by the Pendellösung fringe system can be used as a statistical measure of the degree of lattice imperfection when the lattice imperfections are too small or too numerous to be individually resolved on topographs. Lattice imperfections due to variable impurity content, radiation damage, or fine-scale precipitation fall in this class. When making such measurements it is clearly essential to take into account the minima of fringe visibility that occur using unpolarized X-rays. Hence either the properly computed pattern of superimposed fringes should be used as a standard with which to compare the topographs, or plane-polarized X-rays be used in an experimental arrangement such as that shown in Fig. 2.

*The measurement of F*

It was shown by Kato & Lang (1959) that the measurement of Pendellösung fringe spacings was an accurate method for finding the structure amplitude. Their calculated and observed fringe spacings in various reflexions of silicon and quartz generally agreed well with each other, except that the observed spacings were systematically a few per cent smaller than those calculated using the mean polarization factor. In the present study it has been found that the apparent mean fringe spacing derived from measurements on a train of fringes does depend slightly upon where the beginning and end of the train are situated with respect to the cycle of fringe visibility. Where possible, it is desirable to make measurements on a train of fringes with its first and last fringe separated by an integral number of visibility periods.

We may mention in passing that the conclusion arrived at by Kato & Lang that the structure amplitude of the quartz minor rhombohedron reflexion was in fact 9% higher than the value given by Wei (1935) is confirmed by a comparison with the more recent work of Brill, Hermann & Peters (1942) whose value for this structure amplitude is 10% greater than that of Wei.

*The measurement of  $\kappa$*

Considerable effort has been devoted in recent years to the precise measurement of the transmitted diffracted intensity of various reflexions,  $h$ , from thick specimens of perfect germanium in order to determine  $\kappa = F_h^i/F_h^r$ , or the related quantity  $\varepsilon = F_h^i/F_o^i$  (e.g. Batterman, 1962; Okkerse, 1962; Hildebrandt & Wagenfeld, 1963). Our experiments suggest that provided due account is taken of the superimposition of the separate fringe patterns of  $\sigma$  waves and  $\pi$  waves, analysis of the intensity profiles across topographs of wedges of absorbing crystals should form a simple and quite accurate method of determining  $\kappa$  or  $\varepsilon$ . As already pointed out, the oscillatory components of the integrated reflexion have the normal attenuation coefficient. They could thus serve as an intensity calibration on the topograph which would allow the non-oscillatory terms in equation (4) to be derived easily from the photometric trace. This technique does not require either a stable X-ray source or an electronic X-ray counting system.

The authors gratefully acknowledge financial support from the United Kingdom Department of Scientific and Industrial Research and from the Aerospace Research Laboratories, O.A.R., through the European Office of Aerospace Research, United States Air Force.

**References**

- BATTERMAN, B. W. (1962). *Phys. Rev.* **126**, 1461.  
 BRILL, R., HERMANN, C. & PETERS, C. (1941). *Ann. Phys. Lpz.* **41**, 233.  
 HILDEBRANDT, G. & WAGENFELD, H. (1963). *Acta Cryst.* **16**, A169.  
 JAMES, R. W. (1963). *Solid State Physics*. Vol. 15, p. 53. F. Seitz & D. Turnbull, ed., New York: Academic Press.  
 KATO, N. (1955). *J. Phys. Soc. Japan*, **10**, 46.  
 KATO, N. (1961). *Acta Cryst.* **14**, 526, 627.  
 KATO, N. & LANG, A. R. (1959). *Acta Cryst.* **12**, 787.  
 LANG, A. R. (1959). *Acta Cryst.* **12**, 249.  
 LAUE, M. VON (1960). *Röntgenstrahlinterferenzen*. Frankfurt a/M: Akad. Verlag.  
 OKKERSE, B. (1962). *Philips Res. Rep.* **17**, 464.  
 PARTHASARATHY, R., RAMACHANDRAN, G. N. & MALLIKARJUNAN, M. (1963). *Crystallography and Crystal Perfection*, p. 133. G. N. Ramachandran, ed., New York: Academic Press.  
 RAMACHANDRAN, G. N. (1945). *Proc. Indian Acad. Sci. A*, **39**, 65.  
 WEI, P. (1935). *Z. Kristallogr.* **92**, 355.  
 ZACHARIASEN, W. H. (1945). *Theory of X-ray Diffraction in Crystals*. New York: Wiley.